

Cerebellar Structural Variations in Subjects with Different Hypnotizability

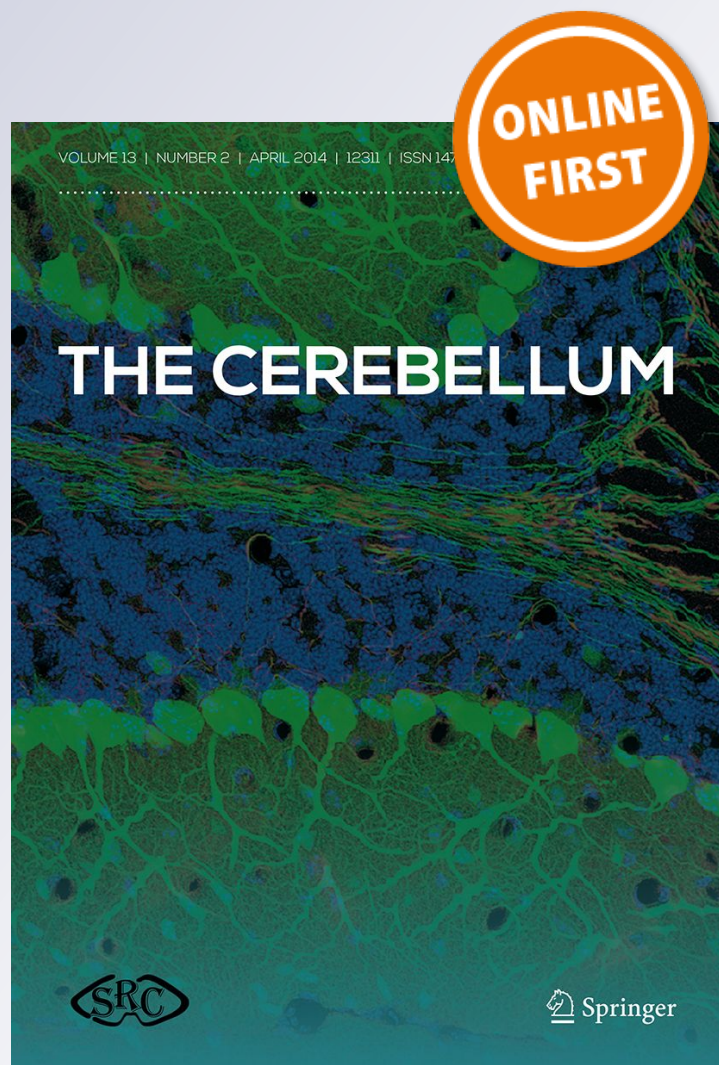
E Picerni, EL Santarcangelo, D Laricchiuta, D Cutuli, L Petrosini, G Spalletta & F Piras

The Cerebellum

ISSN 1473-4222

Cerebellum

DOI 10.1007/s12311-018-0965-y



Your article is protected by copyright and all rights are held exclusively by Springer Science+Business Media, LLC, part of Springer Nature. This e-offprint is for personal use only and shall not be self-archived in electronic repositories. If you wish to self-archive your article, please use the accepted manuscript version for posting on your own website. You may further deposit the accepted manuscript version in any repository, provided it is only made publicly available 12 months after official publication or later and provided acknowledgement is given to the original source of publication and a link is inserted to the published article on Springer's website. The link must be accompanied by the following text: "The final publication is available at link.springer.com".



Cerebellar Structural Variations in Subjects with Different Hypnotizability

E Picerni^{1,2} · EL Santarcangelo³ · D Laricchiuta^{1,2} · D Cutuli^{1,2} · L Petrosini^{1,2} · G Spalletta¹ · F Piras¹

© Springer Science+Business Media, LLC, part of Springer Nature 2018

Abstract

Hypnotizability—the proneness to accept suggestions and behave accordingly—has a number of physiological and behavioral correlates (postural, visuomotor, and pain control) which suggest a possible involvement of cerebellar function and/or structure. The present study was aimed at investigating the association between cerebellar macro- or micro-structural variations (analyzed through a voxel-based morphometry and a diffusion tensor imaging approach) and hypnotic susceptibility. We also estimated morphometric variations of cerebral gray matter structures, to support current evidence of hypnotizability-related differences in some cerebral areas. High (highs, $N = 12$), and low (lows, $N = 37$) hypnotizable healthy participants (according to the Stanford Hypnotic Susceptibility Scale, form A) were submitted to a high field (3 T) magnetic resonance imaging protocol. In comparison to lows, highs showed smaller gray matter volumes in left cerebellar lobules IV/V and VI at uncorrected level, with the results in left lobule IV/V maintained also at corrected level. Highs showed also gray matter volumes smaller than lows in right inferior temporal gyrus, middle and superior orbitofrontal cortex, parahippocampal gyrus, and supramarginal parietal gyrus, as well as in left gyrus rectus, insula, and middle temporal cortex at uncorrected level. Results of right inferior temporal gyrus survived also at corrected level. Analyses on micro-structural data failed to reveal any significant association. The here found morphological variations allow to extend the traditional cortico-centric view of hypnotizability to the cerebellar regions, suggesting that cerebellar peculiarities may sustain hypnotizability-related differences in sensorimotor integration and emotional control.

Keywords Hypnotizability · Cerebellum · Voxel-based morphometry · Diffusion tensor imaging · Individual differences

Introduction

Hypnotizability, or hypnotic susceptibility, is an *individual trait* that predicts the proneness to modify perception, memory, and behavior according to the content of specific suggestions after hypnotic induction [1] and in the ordinary state of consciousness [2]. In healthy subjects, the scores reported on multidimensional hypnotizability scales allow detecting individual differences in the susceptibility to hypnosis and predicting the effects

of suggestions, with high and low hypnotizability scores set at the extremes of a quasi-normal distribution curve with a slight skew and possible bimodality [3, 4].

Hypnotizability is assumed to act on both cognitive and physiological domains, although a unifying mechanism possibly sustaining the double nature of its characteristics has not yet been identified. Indeed, as a cognitive trait, hypnotizability includes components such as imagery [5], fantasy proneness [6], expectancy [7], attention/absorption [8], acquiescence, and consistency motivation [9]. At the same time, as a physiological trait, hypnotizability is characterized by differences in sensorimotor integration, degree of the functional equivalence between imagery and perception, cardiovascular control and brain activity [10]. To this respect, hypnotizability is associated with peculiar cortical EEG activities [11, 12] as well as functional brain characteristics [13–15]. Specifically, functional magnetic resonance imaging (fMRI) studies have indicated that the different levels of hypnotizability are accompanied by variations of activation and/or functional connectivity in the dorsolateral prefrontal cortex, inferior frontal gyrus,

G Spalletta and F Piras contributed equally to this work.

✉ E Picerni
eleonora.picerni@uniroma1.it

¹ I.R.C.C.S. Santa Lucia Foundation, Rome, Italy

² Department of Psychology, University “Sapienza” of Rome, Rome, Italy

³ Department of Translational Research and New Technologies in Medicine and Surgery, Pisa University, Pisa, Italy

dorsal anterior cingulate cortex, and superior parietal region [13, 14, 16–18].

Relatively little (and even conflicting) is known about the brain structural differences between high (highs) and low (lows) suggestible subjects. In highs, there have been described larger anterior part of the corpus callosum [19], larger gray matter (GM) volumes in left superior and middle frontal gyri [17], in left temporo-occipital and inferior parietal cortices, and insula [14], as well as smaller GM volumes in the left superior temporal gyrus and insula [17]. Furthermore, Hoefft and colleagues [16] reported differences between highs and lows in the parietal and temporal regions and even in the cerebellum. Unfortunately, in the latter study GM and white matter (WM) volumes were considered together and the direction of the differences between highs and lows was not clarified. Yet, these cerebellar changes (even if not characterized) appear particularly intriguing. Indeed, plenty of functions notoriously attributed to cerebellar networks have been found to be different in subjects with different hypnotizability levels [10]. In particular, highs differ from lows for a less strict postural control, lower accuracy in visuomotor tasks, higher blink rate and, paradoxically, increased pain intensity and amplitude of cortical responses to nociceptive stimulation after anodal transcranial cerebellar stimulation [10].

On such a basis, we sought to elucidate the cerebellar macro- and micro-structural differences between healthy individuals with high or low hypnotic susceptibility, evaluated by means of Stanford Hypnotic Susceptibility Scale, form A (SHSS-A) [20]. We also estimated morphometric variations of cerebral GM structures, to ascertain whether the eventual hypnotizability-related cerebellar peculiarities were accompanied by differences in other cerebral areas.

At a macro-structural level, we used voxel-based morphometry (VBM) to characterize GM volumetric differences in vivo using a voxel-level approach. At a micro-structural level, we used diffusion tensor imaging (DTI), which supplies reliable physiological information on the direction and degree of water displacement in the brain providing thus information on the obstacles encountered by diffusing water molecules [21, 22]. Among DTI indices, we used mean diffusivity (MD) and fractional anisotropy (FA) as probes for, respectively, GM and WM micro-structural integrity [23–25].

Methods

Participants

Subjects belonging to a large group of healthy volunteers ($N = 100$), submitted to MRI scan protocol for other studies, were enrolled in the present research. Only those who accepted to come again to Santa Lucia Foundation to be tested on

hypnotic susceptibility scale by the evaluator (E.L.S.) were included in the study.

All participants were right-handed as assessed with the Edinburgh Handedness Inventory [26]. The inclusion criteria were age between 18 and 65 years and suitability for MRI scanning. Exclusion criteria included (i) cognitive impairment or dementia, based on Mini Mental State Examination (MMSE) [27] score ≤ 24 [28], identifying positive screening for cognitive deterioration in Italian population, and confirmed by a deeper clinical neuropsychological evaluation by using the Mental Deterioration Battery [29] and NINCDS-ADRDA criteria for dementia [30]; (ii) subjective complaint of memory difficulties or of any other cognitive deficit, interfering, or not with the daily living activities; (iii) major medical illnesses, e.g., diabetes (not stabilized), obstructive pulmonary disease, or asthma; hematologic and oncologic disorders; pernicious anemia; clinically significant and unstable active gastrointestinal, renal, hepatic, endocrine, or cardiovascular system diseases; newly treated hypothyroidism; (iv) current or reported psychiatric (assessed by the SCID-II [31]) or neurological (assessed by a clinical neurological evaluation) disorders (e.g., schizophrenia, mood disorders, anxiety disorders, stroke, Parkinson's disease, seizure disorder, head injury with loss of consciousness, and any other significant mental or neurological disorder); (v) known or suspected history of alcoholism or drug dependence and abuse during lifetime; (vi) MRI evidence of focal parenchymal abnormalities or cerebro-vascular diseases: for each subject, a trained neuroradiologist and a neuropsychologist expert in neuroimaging co-inspected all the available clinical MRI sequences (i.e., T1- and T2-weighted and FLAIR images) to ensure that subjects were free from structural brain pathology and vascular lesions (i.e., FLAIR or T2-weighted hyper-intensities and T1-weighted hypo-intensities).

Behavioral Assessment

Hypnotic Susceptibility

Hypnotic susceptibility assessment was performed through the SHSS-A [20, 32]. According to SHSS-A, individuals with scores ≥ 8 and ≤ 4 out of 12 were considered highs and lows, respectively. The selected participants were 12 highs (4 males; SHSS-A score, (mean \pm SD) 9.4 ± 1.3 ; age, 41.25 ± 12.60 years; range, 21–59; education, 15.58 ± 2.64 years; range, 13–18) and 37 lows (19 males; SHSS-A score, (mean \pm SD) 1.1 ± 1.5 ; age: 40.10 ± 11.74 years; range, 23–62; education, 16.02 ± 3.19 years; range, 8–25). In line with previous researches [16, 19] medium hypnotizable individuals (SHSS-A score 5–7) were not included.

Image Acquisition

Participants underwent the same imaging protocol, which included standard clinical sequences (FLAIR, DP-T2-weighted), a volumetric whole-brain 3D high-resolution T1-weighted sequence and a DTI scan protocol, performed with a 3-T Allegra MR imager (Siemens, Erlangen, Germany). Volumetric whole-brain T1-weighted images were obtained in the sagittal plane using a modified driven equilibrium Fourier transform (MDEFT) sequence (echo time/repetition time—TE/TR—= 2.4/7.92 ms, flip angle 15°, voxel size $1 \times 1 \times 1 \text{ mm}^3$).

Diffusion volumes were acquired by using echo-planar imaging (TE/TR = 89/8500 ms, bandwidth = 2126 Hz/vx; matrix size 128×128 ; 80 axial slices, voxel size $1.8 \times 1.8 \times 1.8 \text{ mm}^3$) with 30 isotropically distributed orientations for the diffusion-sensitizing gradients at one b value of 1000 s mm^2 and two $b = 0$ images. Scanning was repeated three times to increase the signal-to-noise ratio.

All planar sequence acquisitions were obtained in the plane of the anterior-posterior commissure line. Since the posterior cranial fossa usually falls at the lower limit of the field of view, particular care was taken to center subjects' head in the head coil, in order to avoid possible magnetic field dishomogeneities or artifacts at the level of the cerebellum.

Image Processing

T1-weighted and DTI images were submitted to several processing steps. First, to explore the relationship between regional volumes and hypnotic susceptibility on a voxel by voxel basis, T1-weighted images were processed and examined using the SPM12 software (Statistical Parametric Mapping, Institute of Neurology, London, UK), specifically the CAT12 toolbox (C. Gaser, Structural Brain Mapping group, Jena University Hospital, Jena, Germany), running in Matlab R2016a (MathWorks, Natick, MA, USA).

The toolbox extends the unified segmentation model [33] consisting of MRI field intensity inhomogeneity correction, spatial normalization, and tissue segmentation at several pre-processing steps to improve the quality of data pre-processing. Initially, to increase the signal-to-noise ratio in the data, an optimized block wise nonlocal-means filter was applied to the MRI scans using the Rician noise adaption [34]. Then, an adaptive maximum a posteriori segmentation approach extended by partial volume estimation was employed to separate the MRI scans into GM, WM, and cerebro-spinal fluid. The segmentation step was finished by applying a spatial constraint to the segmented tissue probability maps based on a hidden Markov random field model to remove isolated voxels, which were unlikely to be members of a certain tissue class and to close holes in clusters of connected voxels of a certain class. Then, the iterative high-dimensional

normalization approach provided by the Diffeomorphic Anatomical Registration Through Exponentiated Lie Algebra (DARTEL) [35] toolbox was applied to the segmented tissue maps in order to register them to the stereotaxic space of the Montreal Neurological Institute (MNI). The tissue deformations were used to modulate participants' GM and WM maps to be entered in the analyses. Voxel values of the resulting normalized and modulated GM and WM segments indicated the probability (between 0 and 1) that a specific voxel belonged to the relative tissue. After pre-processing (and in addition to visual checks for artifacts), a quality check was performed using CAT12 toolbox to assess the homogeneity of the GM tissues. Finally, the modulated and normalized GM and WM segments were written with an isotropic voxel resolution of 1.5 mm^3 and smoothed with a 8-mm full-width half maximum (FWHM) Gaussian kernel.

The segmented, normalized, modulated, and smoothed GM images were used for neocortical and cerebellar analyses.

Subsequently, DTI images were processed by using FSL 4.1 (www.fmrib.ox.ac.uk/fsl/). As reported above, we focused on MD (in GM) and FA (in WM) measures. MD measures the averaged diffusion of water molecules through tissues. MD increase is associated with states characterized by reduced efficacy of synaptic and extra-synaptic transmission [36]. Accordingly, MD increase in GM has been linked to poor cognitive performance or psychiatric symptoms [37]. FA measures the anisotropy of water diffusion processes in WM. Low FA values stand for isotropic diffusion, while high FA values indicate diffusion fully restricted along one axis, related to fiber density, axonal diameter and myelination [38].

Image distortions induced by eddy currents and head motion in the DTI data were corrected by applying a 3D full affine (mutual information cost function) alignment of each image to the mean no diffusion weighting ($b = 0$) image. After corrections, DTI data were averaged and concatenated into 31 ($1 b_0 + 30 b_{1000}$) volumes. A diffusion tensor model was fit at each voxel and maps of FA and MD were generated. All subjects' FA were non-linearly transformed into standard space using the tool FNIRT [39] and the transformation matrix was then applied to the MD maps which were subsequently smoothed by using a Gaussian kernel with a 6-mm FWHM. We used tract-based spatial statistics (TBSS) [40] version 1.2, part of FSL, for the post processing of FA maps in the so-called WM skeleton, i.e., an alignment invariant tract representation. Briefly, TBSS first projects all subjects' microstructural data onto the skeleton in the standard MNI space by means of the nonlinear registration tool FNIRT [39], which uses a b -spline representation of the registration warp field. This process of projecting individual maps onto a mean skeleton helps to confine the effect of cross-spatial subject variability that remains after classical nonlinear registration. Although the advantages of tractography include overcoming alignment issues by operating in the individual space of

subjects and higher sensitivity in detecting subtle WM microstructural changes, TBSS has been designed to bring together the strengths of both tractography and classic VBM-style approaches. In fact, it is fully automated; it solves the alignment and smoothing problems and investigates the whole WM tissue without the need to pre-specify the tracts of interest [40].

The resulting data are then fed into voxel-wise cross-subject statistics, i.e., the “randomize” command in the FSL package. Analyses restricted to cerebellar and cerebral areas were determined as follows: (1) cerebellar masks were achieved by meaning VBM-based GM or TBSS-based WM probability maps obtained in the processing steps, thresholding the relative image to a value of 0.3 (i.e., removing all voxels having a probability to belong to GM or WM lower or equal to 29%) and manually removing all the non-cerebellar structures using the MNI-oriented atlas of the human brain (Automated Anatomical Labeling Atlas, AAL) [41] as reference; (2) similarly, cerebral masks were achieved by meaning VBM-based GM or TBSS-based WM probability maps obtained in the processing steps, thresholding the relative image to a value of 0.3 (i.e., removing all voxels having a probability to belong to GM or WM lower or equal to 29%) and manually removing the cerebellum using the MNI-oriented atlas of the human brain (Automated Anatomical Labeling Atlas, AAL) [41] as reference. To obtain the precise anatomical localization of results, we superimposed statistical maps onto Diedrichsen's probabilistic atlas of the human cerebellum [42] or onto the AAL template.

Statistical Analysis

The effect of gender in highs and lows was analyzed by means of χ^2 test, while age and education years were assessed by means of unpaired t test. Results of the demographic characteristics were considered significant at the $p < 0.05$ level.

Differences between highs and lows in GM cerebellar and cerebral volumes were tested at the voxel level by means of t tests using CAT12 within the framework of the general linear model (GLM). Total intracranial volume (TIV), age, and education years were used as covariates in the statistical analyses to control for the effects of the sociodemographic variables on the results. Gender was always considered a “dummy variable” given its dichotomic nature.

Significance was corrected through family-wise error (FWE), which controls the possibility of any false positive errors across the entire volume. As preliminary results, we also considered significant those obtained at a more lenient uncorrected threshold of $p < 0.001$. We considered significant only relationships whose voxels were part of a spatially contiguous cluster size of a minimum of 100 voxels.

Differences in DTI data (WM FA and GM MD) between highs and lows were performed through a voxel-wise analysis with the GLM by using the “randomize” program in FSL,

which is an optimized method to detect clusters without having to define clusters in a binary way [43]. The permutation-based non-parametric method with the threshold-free cluster enhancement (TFCE) [44, 45] was used to find significant clusters. Since, to our knowledge, this is the first study assessing the possible relationships between brain microstructure and hypnotizability, for DTI analyses, we accepted an uncorrected statistical level of $p < 0.001$. Mean DTI metrics of significant clusters were extracted to create graphs using *fslmaths* and *fslstats* tools.

Results

Sociodemographic Variables

No significant effect of gender was observed in lows ($\chi^2 = 0.03$; d.f. = 1; $p = 0.87$) and highs ($\chi^2 = 1.33$; d.f. = 1; $p = 0.25$). No significant difference in age ($t = 0.28$; d.f. = 47; $p = 0.77$) and education attainment ($t = -0.43$; d.f. = 47; $p = 0.66$) between highs and lows was found.

Regional Volumes

Cerebellar Regions

Analyses on GM cerebellar volumes revealed a significant difference between highs and lows in left lobules IV/V and left lobule VI, with the highs showing smaller volumes. More importantly, results of left lobules IV/V survived to FWE correction (Fig. 1; Table 1).

Cerebral Regions

At uncorrected threshold, analyses on GM cortical volumes revealed significant differences between highs and lows in right inferior temporal gyrus, middle, and superior orbitofrontal cortex, parahippocampal gyrus and supramarginal parietal gyrus, as well as in left gyrus rectus, insula, and middle temporal cortex, once more with the highs showing smaller volumes than lows. More importantly, results of right inferior temporal gyrus survived to FWE correction (Fig. 2; Table 1).

Micro-structural Measures

As for DTI analyses, no significant difference in GM MD as well as WM FA values was found between groups both in cerebellar and cerebral regions.

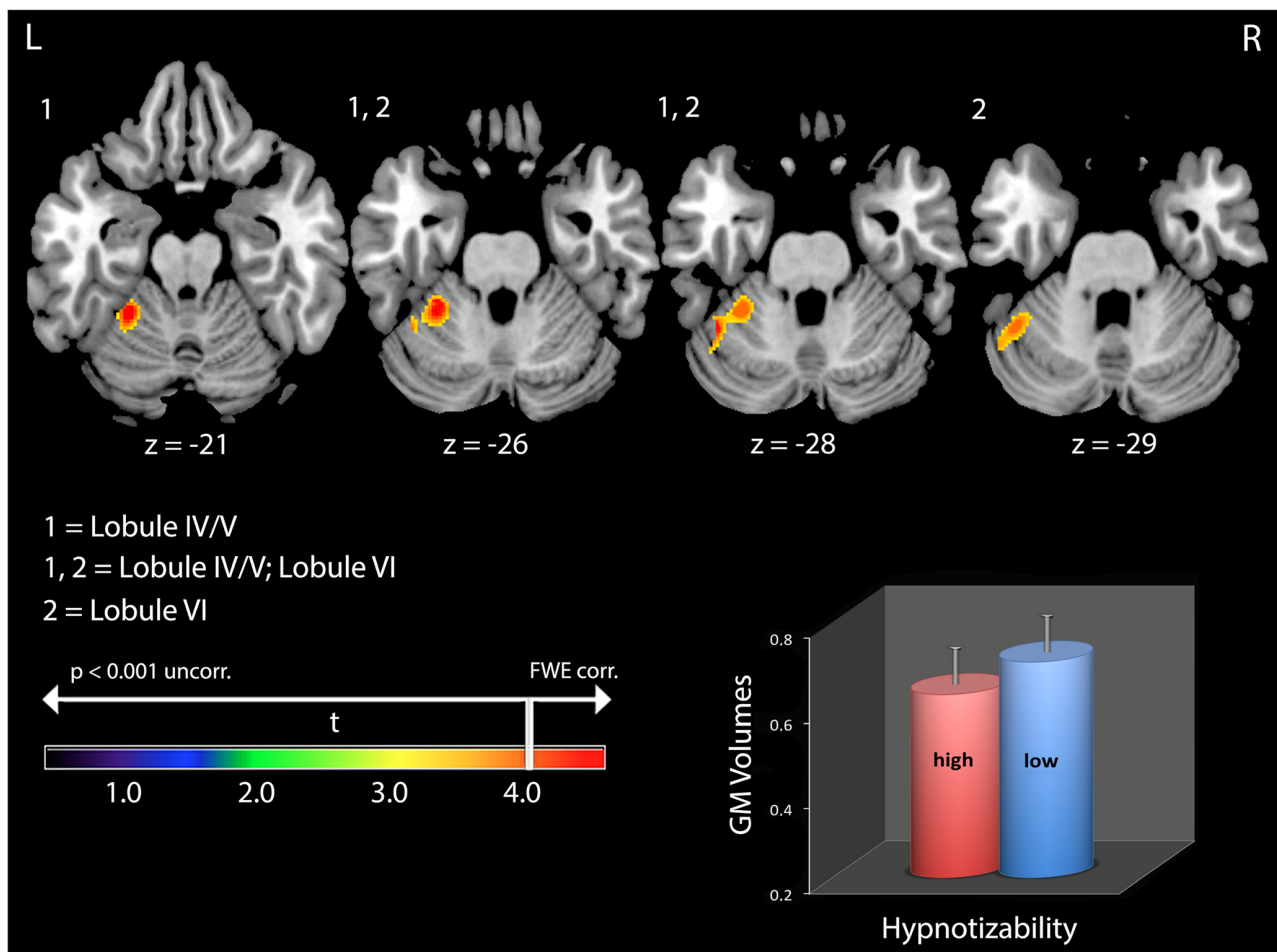


Fig. 1 Gray matter (GM) cerebellar volumes and hypnotic susceptibility scores. Results showed group significant differences (surviving family-wise error correction, FWE, for multiple comparisons) between gray matter cerebellar voxel-based morphometry (VBM) analysis of highs and lows in left lobule IV/V. Above color bars *t* values are indicated. In figure

left, (L) is left and coordinates are in MNI space. Areas significantly associated with hypnotic susceptibility in the voxel-based analyses were used as regions of interest (ROI) to extract raw data and create histograms (mean \pm SEM). Highs: high hypnotizability (SHSS-A scores 8–12) group. Lows: low hypnotizability (SHSS-A scores 0–4) group

Discussion

The present study was aimed at investigating whether eventual structural differences in cerebellar and cerebral regions were linked to the individual differences in hypnotic susceptibility.

The results show that in comparison to lows the highs display significantly smaller GM cerebellar volumes in left lobules IV/V and in left lobule VI. In parallel, the highs have significantly smaller volumes in right inferior temporal gyrus, and at preliminary level, in right middle and superior orbitofrontal cortex, right parahippocampal gyrus, right supramarginal parietal gyrus, left gyrus rectus, left insula, and in left middle temporal cortex. Furthermore, no associations are detected within the DTI micro-structural data. Although the application of a less conservative uncorrected threshold should be viewed with some degree of caution given the risk of false positive results, we decided to consider and

describe also the uncorrected findings given the hypotheses of the study and their potential theoretical significance for further studies.

The present results are in line with most previous findings [17] reporting a widespread GM reduction in highs. Theoretically, the reduction of highs' GM volumes could be read in terms of vascular functional differences. In fact, only in highs the flow-mediated endothelial function related to the release of endothelial nitric oxide (NO) is not reduced by mental stress and nociceptive stimulation [10, 46], suggesting that in highs the vessels are scarcely sensitive to cognitive and sensory stimulation [10]. Intriguingly, the endothelial NO, largely present in the brain in general and in the cerebellum in particular, can diffuse from vessels to neurons [10]. Speculatively, an exaggerated release of endothelial NO, as hypothesized occurring in highs [10], might be detrimental to the neuronal development, thus leading to GM reductions.

Table 1 Comparison between regional gray matter volumes (voxel-based morphometry) of highs and lows

Label for peak	Side	Extent (<i>n</i> voxels)	<i>t</i>	<i>p</i>	equivZ	<i>x</i> , <i>y</i> , <i>z</i> (mm)
Cerebellar lobule IV/V	L	440	4.31	<i>0.022</i>	3.93	−26, −43, −23
Cerebellar lobule VI	L		3.98	0.053	3.66	−40, −51, −27
Temporal inferior gyrus	R	1097	5.42	0.021	4.73	51, −3, −38
Frontal medial orbital	R	348	4.62	0.181	4.15	36, 44, −12
Gyrus rectus	L	146	4.43	0.279	4.02	−12, 34, −18
Parahippocampal gyrus	R	261	4.27	0.389	3.90	26, −16, −20
Frontal superior orbital	R	211	4.25	0.411	3.87	18, 33, −20
Parietal supramarginal gyrus	R	393	4.16	0.483	3.81	56, −39, 28
Insula	L	154	4.09	0.550	3.75	−40, 15, −5
Temporal medial gyrus	L	105	3.87	0.746	3.57	−48, −13, −14

In bold type are reported results surviving at family-wise error (FWE) correction. Coordinates are in Montreal Neurological Institute (MNI) space

L left, *R* right

Nonetheless, we are aware that this hypothesis has to be supported by tailored studies to be validated.

Coming back to the present results, the volumetric differences between highs and lows found in lobules IV/V and VI closely fit with the functional topographic organization of cerebellar regions suggested by their anatomical connectivity with neocortical regions. In fact, the posterior cerebellum (lobules VI and VII, including hemispheric Crus 1 and 2) is retained to be the anatomical substrate of several cognitive functions [47]. It is worth noting that lobule VI represents the anterior boundary between overtly sensorimotor zones (i.e., lobules IV/V) and supra-modal cognitive zones (i.e., lobule VII), so that sensorimotor tasks that involve complex, fast and sequenced movements activate specifically the lobule VI [48]. Thus, the present findings of smaller volumes in lobules IV/V and VI may sustain the previous behavioral observation of altered sensorimotor processing in subjects with high hypnotic susceptibility [10]. It has also been recently reported that the lobule VI, activated by the execution of a motor task with or without verbal encouragement, forms a closed-connectivity loop with orbitofrontal cortex, superior temporal gyrus, and dorsolateral prefrontal cortex via the red nucleus [49]. The structural alteration of orbitofrontal cortex found in the present study is consistent with its involvement in hypnotic susceptibility advanced by the pioneering findings on hypnotic leg paralysis [50].

Left cerebellar IV/V and VI lobules are widely connected with contralateral temporal and parietal cortices, as revealed by resting-state functional connectivity and projection studies [47, 51, 52]. Related to the present topic, the temporal and parietal cortices have been even implicated in individual differences of hypnotic susceptibility or in different facets of hypnotic responding [13, 14]. Further, during hypnotic hyperalgesia altered activity within supramarginal and superior, middle, inferior temporal gyri was described [53].

Intriguingly, although structural variations in the temporal cortex have been associated with hypnotic susceptibility, it is not possible to advance an exhaustive interpretation on the role of temporal cortical circuits in hypnotizability, given some discrepancies on the direction of volumetric changes present in literature [14, 17].

Notably, within the extensive bidirectional cerebello-cortical connections, the lobules IV–VI are even linked to the insular cortex [52, 54]. The current research reveals in highs smaller volumes of left insula. Situated at the intersection of the temporal, parietal, and frontal lobes, the insula represents an integrative center for own-body representation and awareness by receiving large quantities of interoceptive, autonomic, and emotional information from ipsilateral somatosensory and limbic areas, linking them with external elements in order to organize adaptive behaviors [55]. Insular cortex is also involved in self-reflection, self-monitoring, and self-regulation [56], as well as in empathy [57], processes that can be altered in hypnosis [58]. A recent study of functional connectivity has investigated the insular responses to sensory stimuli with affective valence in relation to the individual differences in emotional susceptibility [59]. The study has demonstrated that weaker functional connections of the left anterior insula with left lobule IV were linked to higher emotional susceptibility. Our results on left insular and cerebellar lobule IV peculiarities of highs totally fit with the findings by Ebisch and colleagues [59], suggesting that the changes of these brain structures could represent the correlate of the altered emotional processing reported in highs. In fact, higher emotional intensity during internal imagery [60], sensitivity and empathy [15], tendency to somatic complaints [61], and vividness of pain imagery [46] have been reported in highs. Furthermore, an fMRI study on a sample of highs revealed common activations of the *left* insula and *left* cerebellum, besides prefrontal and parietal cortices, during both hypnotically and physically

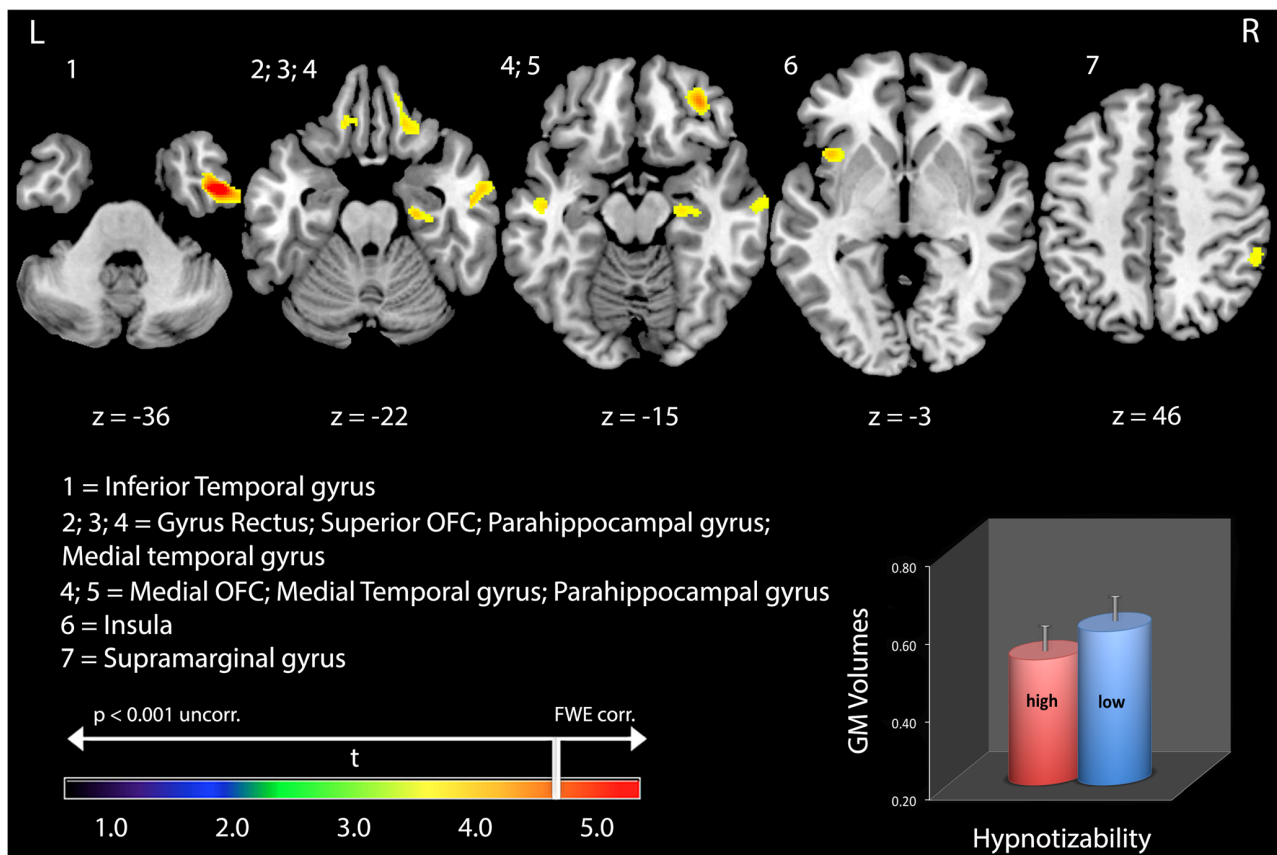


Fig. 2 Gray matter (GM) cortical volumes and hypnotic susceptibility scores. Results showed group significant differences (surviving family-wise error correction, FWE, for multiple comparisons) between gray matter cortical voxel-based morphometry (VBM) analysis of highs and lows in right inferior temporal gyrus. Above color bars t values are indicated. In

figure left, (L) is left and coordinates are in MNI space. Areas significantly associated with hypnotic susceptibility in the voxel-based analyses were used as regions of interest (ROI) to extract raw data and create histograms (mean \pm SEM). Highs: high hypnotizability (SHSS-A scores 8–12) group. Lows: low hypnotizability (SHSS-A scores 0–4) group

induced pain [62]. Thus, in the present study, we found left cerebellar alterations accompanied by both contralateral (right inferior temporal gyrus, middle, and superior orbitofrontal cortex, parahippocampal gyrus, and supramarginal parietal gyrus) and ipsilateral (left gyrus rectus, insula, and middle temporal cortex) cortical alterations. While the former are consistent with the mostly crossed prominent cerebello-cortical projections, the latter although much lesser described have been reported in connectivity and structural studies in humans and animals [63–66]. Accordingly, it is not surprising that not only contralateral but also ipsilateral networks may be sensitive to structural unilateral cerebellar alterations.

Apart from the side of the cerebello-cortical projections, the contribution of cerebellar areas to neocortical processing of hypnotic susceptibility is mediated by bidirectional cerebello-cortical and intra-cortical networks. Increasing evidence emphasizes the role of long-range signals from, and interactions with, associative cortices in the top-down control over lower-level structures [58, 67, 68]. In fact, among the sub-cortical structures, the cerebellum represents the ideal

recipient of cerebral cortex control, since it is broadly involved in the operational processing on information linked to both movement and thought. The cerebellum performs uniform computations on highly specific information received from corresponding “specialized” cortical areas that determine the degree of cerebellar specialization [69]. Internal models (either forward or inverse) are formed in the cerebellum to adapt sensorimotor and cognitive (and even emotional) activities to contextual information [70, 71]. However, as a complementary note, it has to be considered that the top-down processes may (and often do) work in concert with bottom-up mechanisms. The directionality of processing (bottom-up or top-down) could depend on the hierarchical position of the cortical area from which the cerebellum receives its inputs relative to the cortical area to which the cerebellum directs its outputs, placing the cerebellum as a “sub-cortical hub” between hierarchically different cortical regions [72]. Speculatively, the individual differences in hypnotic susceptibility could be mediated by cortico-cerebello-cortical loops in which the sensitivity of some cortical regions might top-down modulate the

activity of cerebellum (lobules IV–VI) which in turn might bottom-up control other cortical regions. We are aware that the distinctive roles of top-down and bottom-up control in hypnotic susceptibility need to be specifically investigated to gain new insight on the physiological mechanisms through which the cerebellar and cortical structural peculiarities may lead to behavioral characteristics.

One of the limitations of the present study is the rather small number of highs enrolled, although it was comparable or even patently superior to that of other imaging reports [14, 16, 17]. By studying a larger sample, highs could be classified according to a more detailed hypnotic profile rather than their mere total hypnotizability scores. This could be useful because different sub-types of highs have been described in relation to their tendency to dissociation, hallucination, and inhibition [73, 74] and such differences may account, for instance, for the scattered brain structural results reported in literature.

Summary

The present findings indicate possible morphological bases for the previously described sensorimotor correlates of hypnotizability [10] and disclose new perspectives in the field of hypnotizability and hypnosis in which the cerebellum might play an intriguing role.

Compliance with Ethical Standards

The Local Ethics Committee of the I.R.C.C.S. Santa Lucia Foundation approved the study and written consent was obtained from all participants after a full explanation of the study procedures. The authors assert that all procedures contributing to this work comply with the ethical standards of the relevant national and institutional committees on human experimentation and with the Helsinki Declaration of 1975, as revised in 2008.

Conflict of Interest The authors declare that they have no conflict of interest.

References

- Elkins GR, Barabasz AF, Council JR, Spiegel D. Advancing research and practice: the revised APA division 30 definition of hypnosis. *Int J Clin Exp Hypn. England.* 2015;63:1–9.
- Meyer EC, Lynn SJ. Responding to hypnotic and nonhypnotic suggestions: performance standards, imaginative suggestibility, and response expectancies. *Int J Clin Exp Hypn. England.* 2011;59:327–49.
- De Pascalis V, Bellusci A, Russo PM. Italian norms for the Stanford hypnotic susceptibility scale, form C. *Int J Clin Exp Hypn. England.* 2000;48:315–23.
- Carvalho C, Kirsch I, Mazzoni G, Leal I. Portuguese norms for the Waterloo-Stanford Group C (WSGC) scale of hypnotic susceptibility. *Int J Clin Exp Hypn. England.* 2008;56:295–305.
- Kogon MM, Jasiukaitis P, Berardi A, Gupta M, Kosslyn SM, Spiegel D. Imagery and hypnotizability revisited. *Int J Clin Exp Hypn. England.* 1998;46:363–70.
- Lynn SJ, Rhue JW. The fantasy-prone person: hypnosis, imagination, and creativity. *J Pers Soc Psychol. United States.* 1986;51:404–8.
- Council JR, Kirsch I, Hafner LP. Expectancy versus absorption in the prediction of hypnotic responding. *J Pers Soc Psychol United States.* 1986;50:182–9.
- Kallio S, Revonsuo A, Hamalainen H, Markela J, Gruzelier J. Anterior brain functions and hypnosis: a test of the frontal hypothesis. *Int J Clin Exp Hypn. England.* 2001;49:95–108.
- Council JR, Green JP. Examining the absorption-hypnotizability link: the roles of acquiescence and consistency motivation. *Int J Clin Exp Hypn. England.* 2004;52:364–77.
- Santarcangelo EL, Scattina E. Complementing the latest APA definition of hypnosis: sensory-motor and vascular peculiarities involved in hypnotizability. *Int J Clin Exp Hypn. England.* 2016;64:318–30.
- Jamieson GA, Burgess AP. Hypnotic induction is followed by state-like changes in the organization of EEG functional connectivity in the theta and beta frequency bands in high-hypnotically susceptible individuals. *Front Hum Neurosci. Switzerland.* 2014;8:528.
- Yargholi E, Nasrabadi AM. Recurrence quantification analysis of electroencephalograph signals during standard tasks of Waterloo-Stanford group scale of hypnotic susceptibility. *J Med Eng Technol. England.* 2015;39:26–34.
- Cojan Y, Pigué C, Vuilleumier P. What makes your brain suggestible? Hypnotizability is associated with differential brain activity during attention outside hypnosis. *Neuroimage [Internet]. Elsevier Inc.;* 2015;117:367–74. Available from: <https://doi.org/10.1016/j.neuroimage.2015.05.076>
- McGeown WJ, Mazzoni G, Vannucci M, Venneri A. Structural and functional correlates of hypnotic depth and suggestibility. *Psychiatry Res - Neuroimaging [internet]. Elsevier;* 2015;231:151–159. Available from: <https://doi.org/10.1016/j.psychres.2014.11.015>
- Facco E, Testoni I, Ronconi L, Casiglia E, Zanette G, Spiegel D. Psychological features of hypnotizability: a first step towards its empirical definition. *Int J Clin Exp Hypn. England.* 2017;65:98–119.
- Hoefl F, Gabrieli JDE, Whitfield-Gabrieli S, Haas BW, Bammer R, Menon V, et al. Functional brain basis of hypnotizability. *Arch Gen Psychiatry United States.* 2012;69:1064–72.
- Huber A, Lui F, Duzzi D, Pagnoni G, Porro CA. Structural and functional cerebral correlates of hypnotic suggestibility. *PLoS One.* 2014;9:e93187.
- Jiang H, White MP, Greicius MD, Waelde LC, Spiegel D. Brain activity and functional connectivity associated with hypnosis. *Cereb Cortex.* 2017;27:4083–93.
- Horton JE, Crawford HJ, Harrington G, Downs JH. Increased anterior corpus callosum size associated positively with hypnotizability and the ability to control pain. *Brain.* 2004;127:1741–7.
- Weitzenhoffer AM, Hilgard E. *Scala Stanford di Suscettibilità Ipnocica, forme A, B. Versione italiana.* Organizzazioni Speciali Firenze; 1959.
- Basser PJ, Pierpaoli C. Microstructural and physiological features of tissues elucidated by quantitative-diffusion-tensor MRI. *J Magn Reson B United States.* 1996;111:209–19.
- Le Bihan D. The “wet mind”: water and functional neuroimaging. *Phys Med Biol. England.* 2007;52:R57–90.
- Laricchiuta D, Petrosini L, Picerni E, Cutuli D, Iorio M, Chiapponi C, et al. The embodied emotion in cerebellum: a neuroimaging study of alexithymia. *Brain Struct Funct.* 2014;

24. Laricchiuta D, Petrosini L, Piras F, Macci E, Cutuli D, Chiapponi C, et al. Linking novelty seeking and harm avoidance personality traits to cerebellar volumes. *Hum Brain Mapp*. 2014;35:285–96.
25. Picerni E, Petrosini L, Piras F, Laricchiuta D, Cutuli D, Chiapponi C, et al. New evidence for the cerebellar involvement in personality traits. *Front Behav Neurosci* [Internet]. 2013;7:133. Available from: <http://www.pubmedcentral.nih.gov/articlerender.fcgi?artid=3788336&tool=pmcentrez&rendertype=abstract>
26. Oldfield RC. The assessment and analysis of handedness: the Edinburgh inventory. *Neuropsychologia* England. 1971;9:97–113.
27. Folstein MF, Folstein SE, McHugh PR. “Mini-mental state”. A practical method for grading the cognitive state of patients for the clinician. *J Psychiatr Res*. England. 1975;12:189–98.
28. Measso G, Zappala G, Cavazzeran F, Crook TH, Romani L, Pirozzolo FJ, et al. Raven’s colored progressive matrices: a normative study of a random sample of healthy adults. *Acta Neurol Scand Denmark*. 1993;88:70–4.
29. Carlesimo GA, Caltagirone C, Gainotti G. The Mental Deterioration Battery: normative data, diagnostic reliability and qualitative analyses of cognitive impairment. The Group for the Standardization of the Mental Deterioration Battery. *Eur Neurol*. Switzerland. 1996;36:378–84.
30. McKhann GM, Knopman DS, Chertkow H, Hyman BT, Jack CRJ, Kawas CH, et al. The diagnosis of dementia due to Alzheimer’s disease: recommendations from the National Institute on Aging-Alzheimer’s association workgroups on diagnostic guidelines for Alzheimer’s disease. *Alzheimers Dement U S*. 2011;7:263–9.
31. First MB, Gibbon M, Spitzer RL, Williams JB. Structured clinical interview for DSM-IV Axis II personality disorders (SCID-II). Washington, DC: American Psychiatric Press; 1997.
32. Weitzenhoffer AM. Hypnotic susceptibility: a personal and historical note regarding the development and naming of the Stanford Scales. *Int J Clin Exp Hypn*. England. 1997;45:126–43.
33. Ashburner J, Friston KJ. Unified segmentation. *Neuroimage*. US. 2005;26:839–51.
34. Wiest-Daessle N, Prima S, Coupe P, Morrissey SP, Barillot C. Rician noise removal by non-local means filtering for low signal-to-noise ratio MRI: applications to DT-MRI. *Med Image Comput Assist Interv*. Germany. 2008;11:171–9.
35. Ashburner J. A fast diffeomorphic image registration algorithm. *Neuroimage* United States. 2007;38:95–113.
36. Sykova E, Nicholson C. Diffusion in brain extracellular space. *Physiol Rev* United States. 2008;88:1277–340.
37. Kantarci K, Senjem ML, Avula R, Zhang B, Samikoglu AR, Weigand SD, et al. Diffusion tensor imaging and cognitive function in older adults with no dementia. *Neurology* United States. 2011;77:26–34.
38. Pierpaoli C, Jezzard P, Basser PJ, Barnett A, Di Chiro G. Diffusion tensor MR imaging of the human brain. *Radiology* United States. 1996;201:637–48.
39. Andersson JLR, Jenkinson M, Smith S. Non-linear registration, aka spatial normalisation. FMRIB Technical Report TR07JA2. Oxford Cent Funct Magn Reson Imaging Brain, Dep Clin Neurol Oxford Univ Oxford, UK. 2007;22.
40. Smith SM, Jenkinson M, Johansen-Berg H, Rueckert D, Nichols TE, Mackay CE, Watkins KE, Ciccarelli O, Cader MZ, Matthews PM, Behrens TEJ. Tract-based spatial statistics: voxelwise analysis of multi-subject diffusion data. *Neuroimage*. United States; 2006;31:1487–1505.
41. Tzourio-Mazoyer N, Landeau B, Papathanassiou D, Crivello F, Etard O, Delcroix N, et al. Automated anatomical labeling of activations in SPM using a macroscopic anatomical parcellation of the MNI MRI single-subject brain. *Neuroimage*. United States. 2002;15:273–89.
42. Diedrichsen J, Balsters JH, Flavell J, Cussans E, Ramnani N. A probabilistic MR atlas of the human cerebellum. *Neuroimage* [Internet]. Elsevier B.V.; 2009 [cited 2014 Jul 11];46:39–46. Available from: <http://www.ncbi.nlm.nih.gov/pubmed/19457380>.
43. Winkler AM, Ridgway GR, Webster MA, Smith SM, Nichols TE. Permutation inference for the general linear model. *Neuroimage* [internet]. The Authors; 2014;92:381–397. Available from: <https://doi.org/10.1016/j.neuroimage.2014.01.060>
44. Nichols TE, Holmes AP. Nonparametric permutation tests for functional neuroimaging: a primer with examples. *Hum Brain Mapp* United States. 2002;15:1–25.
45. Smith SM, Nichols TE. Threshold-free cluster enhancement: addressing problems of smoothing, threshold dependence and localisation in cluster inference. *Neuroimage*. United States. 2009;44:83–98.
46. Scattina E, Huber A, Menzocchi M, Paoletti G, Carli G, Manzoni D, et al. Postural effects of imagined leg pain as a function of hypnotizability. *Exp Brain Res*. Germany; 2012;216:341–348.
47. Stoodley CJ, Schmahmann JD. Evidence for topographic organization in the cerebellum of motor control versus cognitive and affective processing. *Cortex* [Internet]. Elsevier Srl; 2010 [cited 2014 Jul 12];46: 831–44. Available from: <http://www.pubmedcentral.nih.gov/articlerender.fcgi?artid=2873095&tool=pmcentrez&rendertype=abstract>
48. Sauvage C, Jissendi P, Seignan S, Manto M, Habas C. Brain areas involved in the control of speed during a motor sequence of the foot: real movement versus mental imagery. *J Neuroradiol France*. 2013;40:267–80.
49. Belkhiria C, Driss T, Habas C, Jaafar H, Guillemin R, de Marco G. Exploration and identification of cortico-cerebellar-brainstem closed loop during a motivational-motor task: an fMRI study. *Cerebellum* United States. 2017;16:326–39.
50. Halligan PW, Athwal BS, Oakley DA, Frackowiak RS. Imaging hypnotic paralysis: implications for conversion hysteria. *Lancet* (London, England). England; 2000. p. 986–7.
51. O’Reilly JX, Beckmann CF, Tomassini V, Ramnani N, Johansen-Berg H. Distinct and overlapping functional zones in the cerebellum defined by resting state functional connectivity. *Cereb Cortex* [Internet]. 2010 [cited 2014 Jul 30];20:953–65. Available from: <http://www.pubmedcentral.nih.gov/articlerender.fcgi?artid=2837094&tool=pmcentrez&rendertype=abstract>
52. Sultan F, Augath M, Hamodeh S, Murayama Y, Oeltermann A, Rauch A, Thier P. Unravelling cerebellar pathways with high temporal precision targeting motor and extensive sensory and parietal networks. *Nat Commun* [Internet]. Nat Publ Group; 2012;3:924. Available from: <https://doi.org/10.1038/ncomms1912>
53. De Pascalis V, Russo E. Hypnotizability, hypnosis and prepulse inhibition of the startle reflex in healthy women: an ERP analysis. *PLoS One*. 2013;8:e79605.
54. Cauda F, Costa T, Torta DME, Sacco K, D’Agata F, Duca S, et al. Meta-analytic clustering of the insular cortex: characterizing the meta-analytic connectivity of the insula when involved in active tasks. *Neuroimage*. United States. 2012;62:343–55.
55. Craig ADB. Significance of the insula for the evolution of human awareness of feelings from the body. *Ann N Y Acad Sci*. United States. 2011;1225:72–82.
56. Herwig U, Kaffenberger T, Schell C, Jancke L, Bruhl AB. Neural activity associated with self-reflection. *BMC Neurosci*. England. 2012;13:52.
57. Gu X, Gao Z, Wang X, Liu X, Knight RT, Hof PR, et al. Anterior insular cortex is necessary for empathetic pain perception. *Brain* England. 2012;135:2726–35.
58. Terhune DB, Hedman LRA. Metacognition of agency is reduced in high hypnotic suggestibility. *Cognition* Netherlands. 2017;168: 176–81.
59. Ebisch SJH, Bello A, Spitoni GF, Perrucci MG, Gallese V, Committeri G, Pastorelli C, Pizzamiglio L. Emotional susceptibility trait modulates insula responses and functional connectivity in

- flavor processing. *Front Behav Neurosci* [Internet] 2015;9:1–14. Available from: <https://doi.org/10.3389/fnbeh.2015.00297>
60. Kirenskaya AV, Novototsky-Vlasov VY, Chistyakov AN, Zvonikov VM. The relationship between hypnotizability, internal imagery, and efficiency of neurolinguistic programming. *Int J Clin Exp Hypn*. England. 2011;59:225–41.
 61. Younger JW, Rossetti GC, Borckardt JJ, Smith AR, Tasso AF, Nash MR. Hypnotizability and somatic complaints: a gender-specific phenomenon. *Int J Clin Exp Hypn*. England. 2007;55:1–13.
 62. Derbyshire SWG, Whalley MG, Stenger VA, Oakley DA. Cerebral activation during hypnotically induced and imagined pain. *NeuroImage*. 2004;23:392–401.
 63. Schmahmann JD, Pandya DN. Prefrontal cortex projections to the basilar pons in rhesus monkey: implications for the cerebellar contribution to higher function. *Neurosci Lett*. 1995;199:175–8.
 64. Allen G, McColl R, Barnard H, Ringe WK, Fleckenstein J, Cullum CM. Magnetic resonance imaging of cerebellar-prefrontal and cerebellar-parietal functional connectivity. *Neuroimage*. 2005;
 65. Oulad Ben Taib N, Manto M. Reinstating the ability of the motor cortex to modulate cutaneomuscular reflexes in hemispherectomized rats. *Brain Res*. 2008;
 66. Olivito G, Dayan M, Battistoni V, Clausi S, Cercignani M, Molinari M, et al. Bilateral effects of unilateral cerebellar lesions as detected by voxel based morphometry and diffusion imaging. *PLoS One*. 2017;
 67. Gazzaley A, D'Esposito M. Top-down modulation and normal aging. *Ann N Y Acad Sci*. United States. 2007;1097:67–83.
 68. Lynn SJ, Boycheva E, Barnes S. To assess or not assess hypnotic suggestibility? That is the question. *Am J Clin Hypn* United States. 2008;51:161–84.
 69. Ito M. Control of mental activities by internal models in the cerebellum. *Nat Rev Neurosci* England. 2008;9:304–13.
 70. Synofzik M, Lindner A, Thier P. The cerebellum updates predictions about the visual consequences of one's behavior. *Curr Biol* England. 2008;18:814–8.
 71. Ito M. Error detection and representation in the olivo-cerebellar system. *Front Neural Circuits*. Switzerland. 2013;7:1.
 72. Kellermann T, Regenbogen C, De Vos M, Mossnang C, Finkelmeyer A, Habel U. Effective connectivity of the human cerebellum during visual attention. *J Neurosci*. 2012;32:11453–60.
 73. Terhune DB, Cardena E, Lindgren M. Dissociative tendencies and individual differences in high hypnotic suggestibility. *Cogn Neuropsychiatry* England. 2011;16:113–35.
 74. Terhune DB, Cardena E. Heterogeneity in high hypnotic suggestibility and the neurophysiology of hypnosis. *Neurophysiol Clin*. 2015;45:177–8.